

## Triple quantum dot charging rectifier

A. Vidan and R. M. Westervelt<sup>a)</sup>

Division of Engineering and Applied Sciences and Department of Physics, Harvard University, Cambridge, Massachusetts 02138

M. Stopa

Tarucha Mesoscopic Correlation Project, ERATO-JST NTT Atsugi Research and Development Laboratories, Atsugi, Japan

M. Hanson and A. C. Gossard

Materials Department, University of California, Santa Barbara, California 93106

(Received 16 June 2004; accepted 12 August 2004)

Three tunnel-coupled quantum dots in the Coulomb blockade regime act as a molecular rectifier. We have realized this device in a GaAs/Al<sub>0.3</sub>Ga<sub>0.7</sub>As heterostructure containing a two-dimensional electron gas using lithographically patterned gates. The current through two tunnel-coupled dots in series is recorded versus applied voltage. Ratchet behavior is created by a third dot, with one lead, tunnel-coupled to one of the two dots. An electron enters the third dot where it is trapped, producing a jamming effect where no other electron may enter the device. The current–voltage characteristics show rectification and negative resistance arising from charging of the third dot. © 2004 American Institute of Physics. [DOI: 10.1063/1.1807030]

Electron transport of coupled quantum dots in the Coulomb blockade regime, of both serial and parallel configurations,<sup>1–3</sup> has been studied extensively. While single quantum dots can be considered as “artificial atoms,”<sup>4</sup> coupled quantum dots can be considered as “artificial molecules.” Interactions between dots, caused by interdot tunneling or capacitive coupling, give rise to changes in the conductance spectra and current–voltage characteristics of the system. Recently, it has been shown that Coulomb interaction between dots can give rise to ratchet effects.<sup>5</sup> The Coulomb blockade formalism,<sup>6</sup> used to describe single-electron charging and transport through a multiple quantum dot system, can be used to predict these new ratchet effects. Work with quantum dots displaying ratchet behavior has been explored both experimentally and theoretically.<sup>7,8</sup> In this letter, we present an experimental realization of a triple quantum dot rectifier, or Coulomb blockade charging ratchet, as proposed in Ref. 5. Here, three quantum dots are arranged in an *asymmetric* configuration such that a rectifying effect, characteristic of ratchet behavior,<sup>9</sup> is observed.

Figure 1(a) shows a scanning electron micrograph of the triple quantum dot charging ratchet. Fifteen independently tunable Cr: Au gates are used to define three coupled quantum dots in a GaAs/Al<sub>0.3</sub>Ga<sub>0.7</sub>As heterostructure containing a two-dimensional electron gas (2DEG) located 57 nm below the surface. At 4 K, the 2DEG sheet carrier density and mobility are  $n_s = 4.5 \times 10^{11} \text{ cm}^{-2}$  and  $\mu = 400\,000 \text{ cm}^2 \text{ V}^{-1} \text{ s}^{-1}$ . The three dots are arranged in a ring structure, with tunneling possible between dots 1 and 2 and dots 1 and 3. Tunneling is forbidden between dots 2 and 3. A finite-bias Coulomb blockade measurement of dot 2 is shown in Fig. 2, from which we can deduce the total dot capacitance to be  $C_2 \sim 310 \text{ aF}$ . All measurements were done in a Helium-3 system at the base temperature 380 mK and measured electron temperature 440 mK.

The ratchet mechanism observed in this triple quantum dot is a bias-dependent current rectification,<sup>5</sup> similar to the effect seen with a hybrid molecular electronic device.<sup>10</sup> As is typical for a ratchet, breaking of symmetry under inversion must be present, and is introduced here by placing an infinite barrier between dots 2 and 3. Because no tunneling takes place between dots 2 and 3, dot 3 is a quantum box that is tunnel-coupled with dot 1. Dot 2 and dot 3 are now only capacitively coupled. From the circuit model of the triple quantum dot shown in Fig. 1(b), we are able to plot the stability diagram of the system,<sup>11</sup> as is routinely done for double quantum dots.<sup>2,12</sup> The stability diagram displays a “quadruple point,” analogous to the triple point of a double dot system, where four states are degenerate. These four states correspond to no *excess* electrons in the system or one *excess* electron on one of the three dots. Therefore, the triple dot can be tuned such that *zero* or *only one* excess electron is

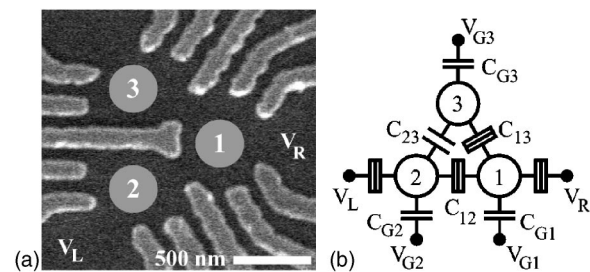


FIG. 1. (a) Scanning electron micrograph of the triple quantum dot. The light areas are Cr: Au gates used to define the quantum dots. The locations of the dots are highlighted by circles. This geometry allows for tunneling between dots 1 and 2, and between dots 1 and 3. Dots 2 and 3 are capacitively coupled, but no electrons may tunnel between these dots. (b) Circuit diagram of a triple quantum dot, with source-drain voltage  $V_{SD} = V_L - V_R$ . Split boxes represent tunnel junctions with capacitance  $C_L$ . Each quantum dot ( $i=1,2,3$ ), with total capacitance  $C_i$ , has its own independent capacitively coupled side gate, with gate voltage  $V_{Gi}$  and capacitance  $C_{Gi}$ . Cross-capacitances are neglected. Interdot and dot-lead tunnel junctions are modeled as a large resistor and capacitor in parallel. An asymmetry is introduced by not permitting any transfer of charge between dot 2 and dot 3:  $C_{23}$  is a pure capacitor.

<sup>a)</sup>Electronic mail: westervelt@deas.harvard.edu

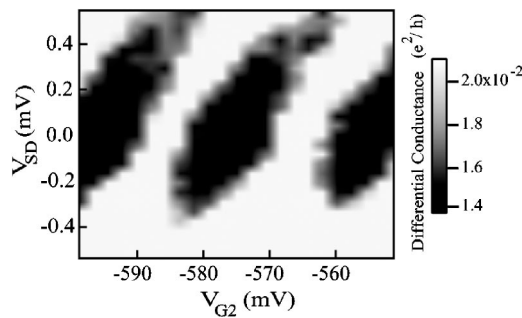


FIG. 2. Differential conductance of dot 2 as a function of its side gate voltage and the dc bias. The diamonds are Coulomb blocked regions from which we measure the total dot capacitance  $C_2 \sim 310$  aF.

allowed in the device. This is crucial for the operation of a triple dot as a charging ratchet. At the quadruple point, a current can flow if electrons tunnel through the device *one at a time*. For small source–drain voltage, while operating the device at the quadruple point, the energy of all four states is degenerate, and an electron can tunnel from the source to the drain through multiple tunneling events between all three dots. However, as the source–drain voltage is increased, the degeneracy of the quadruple point is broken, and if an electron tunnels into the quantum box, dot 3, it gets trapped there, and prohibits the flow of current. For reverse bias no trapping occurs. It was shown<sup>5</sup> that the current through the triple dot is inversely proportional to the trapping ratio  $\gamma_{3\leftarrow 1}/\gamma_{1\leftarrow 3}$ , where  $\gamma_{j\leftarrow i}$  is the rate of tunneling from *dot i* to *dot j*. Furthermore, using the orthodox theory of the Coulomb blockade

$$\gamma_{3\leftarrow 1}/\gamma_{1\leftarrow 3} = e^{\Delta F_{13}/k_B T}, \quad (1)$$

where  $k_B$  is Boltzmann's constant,  $T$  is the temperature, and  $\Delta F_{13}$  is the change in global free energy of the system when a tunneling event between dot 1 and dot 3 occurs, and is linearly proportional to the source–drain voltage  $V_{SD}$ . We then have that for increased  $V_{SD}$ , trapping dominates, and the current is rectified. For reverse biasing, no trapping occurs, and the current is not suppressed.

We operate the triple dot device in the Coulomb blockade regime. We are able to tune the device to the quadruple point by (i) energizing all the gates to deplete the electron gas underneath to form three open quantum dots; (ii) independently tuning each dot to the tunneling regime and then to a Coulomb blockade peak; (iii) returning all fifteen gates to the values found in the previous step; (iv) pinching off the lead to dot 3, thereby forming a quantum box. We measure a dc current  $I$  from an applied source–drain voltage  $V_{SD}$  across dots 1 and 2.

Current–voltage ( $I$ – $V$ ) characteristics of the triple dot charging rectifier are shown in Fig. 3, including polynomial interpolation of the data. The  $I$ – $V$  characteristics show the rectification effect due to the charging of the quantum box, i.e., trapping an electron in dot 3. The ratchet behavior expected is clearly observed: (i) for  $V_{SD} < 0$ , current flows through the device; (ii) for  $V_{SD}$  near zero, the current is symmetric; (iii) as  $V_{SD}$  is made more positive, trapping in dot 3 dominates, and the current is rectified; (iv) as  $V_{SD}$  is further increased, the rectification effect is overcome. Properties (i) and (iii) follow from Eq. (1) directly. Property (ii) is a direct consequence of operating the triple dot at the quadruple point where the four allowed states of the system are degenerate.

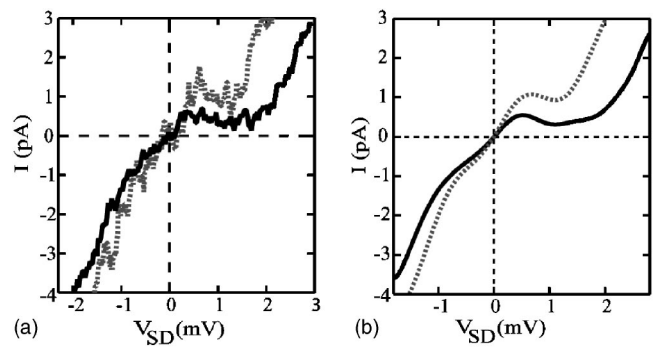


FIG. 3. (a)  $I$ – $V$  characteristics of the triple quantum dot. The dotted (solid) line corresponds to weaker (stronger) coupling between dots 2 and 3, which gives rise to weaker (stronger) current suppression for forward bias. (b) Polynomial interpolation of the data in (a).  $I(V)$  is symmetric around  $V_{SD} = 0$  for both curves, which is a distinct feature of operating at the quadruple point. The region of negative differential resistance for  $V_{SD} > 0$  is clearly observed.

Property (iv) is a result of the high source–drain voltage pushing the system away from the quadruple point and allowing for more than one electron in the system at a given time. Negative resistance is also observed in the  $I$ – $V$  characteristics, and is seen clearly in Fig. 3(b).

Monte Carlo simulations of the  $I$ – $V$  characteristics of our device, employing capacitances derived from the self-consistent simulation of the full three-dimensional structure, including wafer profile and the device surface gate pattern, are shown in Fig. 4.<sup>5,13</sup> The simulations show that the capacitance of a single dot is of order 280 aF, similar to the value extracted from the Coulomb blockade diamond of Fig. 2. The resumption of current at the edge of the suppression region for positive  $V_{SD}$  requires the addition of a second excess electron to the dot system. Analytically, the condition for this second electron entry gives a source–drain voltage threshold  $V_{SD} = e[C_a^{-1}]_{13}/(1 + [C_a^{-1}]_{11}C_{1,L1})$ , where  $e$  is the electron charge,  $C_a$  is the capacitance submatrix between the three dots, and  $C_{1,L1}$  is the capacitance between the first lead and the first dot. This requires that we assume a smaller trapping dot in order to obtain a suppression region comparable to experiment. This is reasonable considering that the trapping dot is acting as a quantum box with only one lead.

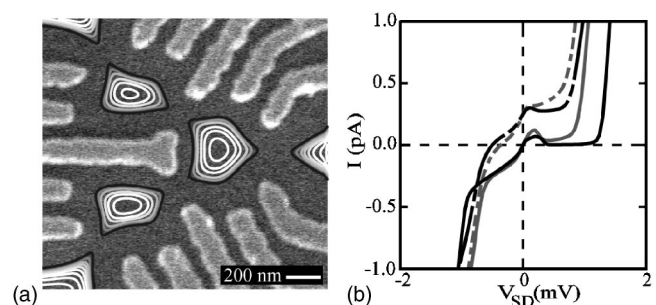


FIG. 4. (a) Potential contours from a self-consistent electronic structure simulation of the triple quantum dot shown in Fig. 1(a). Dots are formed within contours that range from approximately  $-12$  meV at the center of the dots to zero. This simulation is used to extract realistic values for total dot capacitances and interdot capacitances. (b) Monte Carlo simulations of the  $I$ – $V$  characteristics for the triple dot rectifier. Dashed lines are simulated at  $T=450$  mK and solid lines at  $T=350$  mK. From the bottom for  $V_{SD} > 0$ :  $C_1=C_2=210$  aF,  $C_3=50$  aF;  $C_1=C_2=280$  aF,  $C_3=50$  aF;  $C_1=C_2=280$  aF,  $C_3=105$  aF,  $C_{23}=50$  aF;  $C_1=C_2=280$  aF,  $C_3=105$  aF,  $C_{23}=33$  aF; the upper two curves are offset vertically by 0.25 pA for clarity.

Junction resistances were used to fit the overall current range in the Ohmic regime for negative bias.

The measured  $I$ - $V$  characteristics in Fig. 3 and the simulations in Fig. 4 show that the rectification effect is tunable, depending on the capacitive-coupling  $C_{23}$  between dots 2 and 3. We are able to decrease  $C_{23}$  while maintaining approximately constant junction resistances by applying a more negative voltage on the center gate, while raising the voltage on the two opposite interdot quantum point contact gates. Figure 3 shows two  $I$ - $V$  curves for our device under weak and strong capacitive coupling of dots 2 and 3. For larger  $C_{23}$ , stronger rectification is observed, as predicted by the Monte Carlo simulations. The simulations verify the features seen in the data, including the crossing of the two curves at  $V_{SD}=0$ .

In conclusion, we have presented an experimental realization of a triple quantum dot charging ratchet. Recently, a spin-Coulomb blockade rectifier using a double quantum dot has been realized.<sup>14</sup> Both of these devices act as molecular rectifiers for electrons, furthering the analogy between coupled quantum dots and artificial molecules.

The authors would like to acknowledge S. Valenzuela for experimental assistance. This work was supported at Harvard by DARPA DAAD19-01-1-0659, and at UCSB by iQUEST.

<sup>1</sup>L. P. Kouwenhoven, C. M. Marcus, P. McEuen, S. Tarucha, R. M. Westervelt, and N. Wingreen, in *Mesoscopic Electron Transport*, edited by L. L. Sohn, L. P. Kouwenhoven, and G. Schön (Kluwer, Dordrecht, 1997), p. 105.

<sup>2</sup>W. G. van der Wiel, S. De Franceschi, J. M. Elzerman, T. Fujisawa, S. Tarucha, and L. P. Kouwenhoven, *Rev. Mod. Phys.* **75**, 1 (2003), and references therein.

<sup>3</sup>C. Livermore, C. H. Crouch, R. M. Westervelt, K. L. Campman, and A. C. Gossard, *Science* **274**, 1332 (1996); I. H. Chan, R. M. Westervelt, K. D. Maranowski, and A. C. Gossard, *Appl. Phys. Lett.* **80**, 1818 (2002).

<sup>4</sup>M. A. Kastner, *Phys. Today* **46**, 24 (1993).

<sup>5</sup>M. Stopa, *Phys. Rev. Lett.* **88**, 146802 (2002).

<sup>6</sup>*Single Charge Tunneling*, edited by H. Grabert and M. H. Devoret (Plenum, New York, 1992).

<sup>7</sup>H. Linke, W. Sheng, A. Lofgren, H. Xu, P. Omling, and P. E. Lindelof, *Europhys. Lett.* **44**, 341 (1998).

<sup>8</sup>H. Linke, T. E. Humphrey, A. Lofgren, A. O. Sushkov, R. Newbury, R. P. Taylor, and P. Omling, *Science* **286**, 2314 (1999).

<sup>9</sup>For a review, see P. Reimann, *Phys. Rep.* **361**, 57 (2002).

<sup>10</sup>C. Joachim, J. K. Gimzewski, and A. Aviram, *Nature (London)* **408**, 541 (2000).

<sup>11</sup>The electrostatic energy of the triple dot (for negligible cross-capacitances and zero source-drain voltage) is  $U(N_1, N_2, N_3) = \sum_{i=1}^3 (1/2) E_i N_i^2 + \sum_{i<j=2}^3 N_i N_j E_{ij} + f(V_{G1}, V_{G2}, V_{G3})$  with  $f(V_{G1}, V_{G2}, V_{G3}) = (1/2e^2) \sum_{i=1}^3 (C_{Gi}^2 V_{Gi}^2 E_i - 2e C_{Gi} V_{Gi} E_i N_i) + (1/e^2) \sum_{i<j=2}^3 C_{Gi} V_{Gi} C_{Gj} V_{Gj} E_{ij} - (1/e) \sum_{i \neq j} C_{Gi} V_{Gi} E_{ij} N_j$  and  $E_i$  being the charging energy of the dot  $i$  and  $E_{ij}$  is the electrostatic coupling energy between dots  $i$  and  $j$  in the presence of dot  $k$ , given by  $E_i = (e^2/C_i) [1 - (2C_{12}C_{13}C_{23} + C_j C_{ik}^2 + C_k C_{ij}^2) / (C_1 C_2 C_3 - C_i C_{jk}^2)]^{-1}$  and  $E_{ij} = e^2 (C_{ij} C_k + C_{ik} C_{jk}) / (C_1 C_2 C_3 - 2C_{12} C_{13} C_{23} - C_1 C_{23}^2 - C_2 C_{13}^2 - C_3 C_{12}^2)$ . The stability diagram can then be plotted, see A. Vidan, R. M. Westervelt, M. Stopa, M. Hanson, and A. C. Gossard, *J. Supercond.* (in press).

<sup>12</sup>H. Pothier, P. Lafarge, C. Urbina, D. Esteve, and M. H. Devoret, *Europhys. Lett.* **17**, 249 (1992); I. M. Ruzin, V. Chandrasekhar, E. I. Levin, and L. I. Glazman, *Phys. Rev. B* **45**, 13469 (1992).

<sup>13</sup>M. Stopa, *Phys. Rev. B* **54**, 13767 (1996).

<sup>14</sup>K. Ono, D. G. Austing, Y. Tokura, and S. Tarucha, *Science* **297**, 1313 (2002).